Computer & Robotics

Visual Torch Position Control Using Fuzzy-Servoing Controller for Arc Welding Process

Reza Babazadeh Tili [a,*], Fereshteh Akbarnejad [b], Vahid Rostami [c]

[a] *Faculty of Electrical, Biomedical and Mechatronics Engineering, Qazvin Branch, Islamic Azad University, Qazvin, Iran*
[b] *Faculty of ergonomics- University of Social Welfare and Rehabilitation sciences (USWR), USWR, Koodakyar Dead end, Daneshjoo Blvd, Evin, Tehran, Iran*
[c] *Faculty of Computer and Information Technology Engineering, Qazvin Branch, Islamic Azad University, Qazvin, Iran*

Received 15 December 2016; revised 21 September 2017; accepted 11 October 2017; available online 15 March 2018

Abstract

In this paper, we propose a fuzzy-servoing controller method for automatic welding. The proposed method uses a vision based arc tracking to find the initial points of the weld seam and to track them without a prior knowledge. Due to a serious melt down in the weld pool during the welding process, the method requires to control the welding torch in two directions, up-down and left-right directions. To perform these, an IR, two CCD cameras and two stepper motors by inference of fuzzy rules are used to control the movement of the welding torch tip. Therefore, the proposed method can accomplish different tasks such as welding a curved seam or moving into multi directions, while majority of autonomous arc-welding approaches are single-purpose so that they are designed to accomplish only one task, like welding in a direct line or a predefined arc seam. This method is applied on several workpieces and then the maximum error in both directions is shifted to zero in 30ms. This time is proper for workpieces with thickness in the range of [1-5] mm.

Keywords: *Welding Automation, Welding Control, Welding Quality Control, Machine Vision.*

1. Introduction

Arc welding is one of the most feasible methods in joining metallic parts to each other. Arc welding produces fortified and high quality joints [1]. In dangerous places such as nuclear reactors [2], construction industries, [3] and shipbuilding manufacturing [3-5] arc welding was applied as a reliable method of welding. Welding by means of a spark discharge is a process that occurs between two electrodes when the electric field strength, in volts per centimetre, surpasses a certain threshold value; which increases the ion concentration between two electrodes that causes an impermanent phenomenon, causing the air between two electrodes to act as a conductor [6]. In addition, if the spark discharge continues, it will produce an arc, which is used in several processes, including Electro Discharge Machinery (EDM), mass spectrometry, and arc welding. However, there are some serious problems with arc welding, such as aligning the welding torch tip with the center of the welding seam at the initial point [1], continuing welding process on the seam center_ called seam tracking [4, 7, 8]. And weld pool temperature control issues [9]. Aligning the welding torch tip at the initial point, continuing welding process on the seam center and weld pool temperature control are basic problems in the face of automatic welding machinery. Some approaches

* Corresponding author. Email: R.babazadeh@qiau.ac.ir

focused on one of the problems, and some others applied a vision system using template matching to overcome the problems. In these approaches, more welding knowledge of the heat control _as well as image sampling of the welding seam_ is required.

To overcome some of these issues, J.Le et.al, [10] have worked on a circular shaped welding process by means of rotating arc censors. Their research is applicable for cylindrical-shaped workpieces and rotating shapes. Nevertheless, it cannot be applied on workpieces with direct shapes. Zhu et.al, [11] worked on initial weld torch positioning and seam tracking. In order to find the correct position of the welding torch tip, they used a template matching method which transforms 2D images to 3D. In order to align the welding torch tip to the welding seam center, Chen et.al, [12] used the same method for pattern matching algorithm, one of the problems of their system is that a large data base is required for the matching process, and collecting information for all types of welding cannot be accessible for all types of workpieces; Sateesh et.al, [13] proposed an automatic arc welding machine, which is controlled by a fuzzy controller, which is only applicable on weld seams with a direct pattern. Wang et.al, [14] developed a weld seam detection method using template matching algorithm to align the torch tip with the center of the welding seam. Chen et.al, [7] has proposed a three dimensional weld seam modeling. They also used the seam tracking method, which is applied by a self-teaching model on a six-degree-of-freedom robot using inverse kinematics. Although their robot has a sufficient DOF, the control principle might be complicated and the decision-making process of their TSK fuzzy controller cannot cover all types of workpieces. Zhou et.al, [15] introduced a training method for welding robots to perform the welding process on different workpieces. They employed two CCD cameras, one for seam tracking and the other one for the weld quality control, seam tracking from one direction cannot guarantee the weld thickness and its alignment with the seam in all directions, also, they cannot monitor the weld pool temperature for delicate workpieces by means of a CCD camera; therefore, their mechanism might not be applicable for workpieces with various thicknesses. Zhau's method is suitable for manufacturing systems, which manufacture a constant workpiece. Yan et.al, [16] introduced a visual-servoing method, which used a laser diode to assist the seam tracking, but the laser diode needs to move accordingly with respect to the weld torch to be able to work multi directional. Shen et.al [17] addressed a real-time seam-tracking and weld pool control method. In order to extract the welding seam feature lines, they employed two mirrors. This employment restricts the movement of the welding torch along with the curve-shaped seams. In some cases, such as variation in width or depth of the workpiece, their system has to be calibrated. Y. Bazargan-Lari et.al [18] have developed a welding mechanism using SCARA robot to perform Gas Metal Arc Welding (GMAW) process; they have designed two controllers to accurately accomplish the process. Xu et.al, [19] also used a laser diode to aid a better seam tracking. In order to obtain the best weld quality, Chokkalingham et.al, [9] and Gao et.al, [20] have used an infrared (IR) sensor to estimate the weld pool temperature. Satheesh et.al, [13] worked on a fuzzy-controlled welding machine. Dong et.al, [21] addressed initial point and Seam tracking problems for the visual-servoing strategies. They also addressed the problems of vision systems for not being able to capture appropriate pictures. Consequently, in most of these systems, the welding process has to stop at specific places. And, because of the uniformity of the welding seam, the process speed has to be controlled and has to remain unchanged [1, 16].

The aim of this paper is to present a visual-servoing controller based on fuzzy rules to find the initial point of the weld seam, and track the seam automatically. In this method, an error detection algorithm computes the amount of welding torch adjustments in both directions (up/down and left/right). Then, a fuzzy controller, using the errors and its proper derive, obtains the output signals for two stepper motors. The stepper motors can drive the welding torch tip to the desired place. In order to prevent melting in workpieces with a lower thickness, the melt pool temperature has to be controlled, though the temperature control was not typically applied in traditional welding processes. In the traditional method, distance between the torch tip and the work piece is controlled manually to prevent melting. In the proposed method, the stepper motor 1 controls the welding torch tip upward and downward (between 1 to 8 millimetres, depending on the workpiece thickness). Stepper motor 2 controls the welding torch tip in the right and left directions.

2. Methodology

Monitoring the welding seam is a challengeable process; various methods and applications were proposed to overcome this issue. However, MATLAB image processing toolbox provides us with useful tools and algorithms to perform image processing applications with a higher accuracy and reliability. Therefore, we used this software for all of the image processing tasks in this study.

Basically, it is necessary to detect the welding seam, and then define the center of the seam. Accordingly, the welding seam center is computed between two feature lines using Sobel edge detection and Hough transform line extraction algorithms [3, 22]. The controller attempts to align the welding torch above the seam center. In addition, to avoid the workpiece melting, the weld pool temperature is controlled by means of an IR detector. IR sensor transfers images to the image processing algorithm for further considerations. IR sensor is also used to detect the welding seam when the environment light is not sufficient.

Secondly, a control principle was designed to manipulate the welding process with a higher accuracy using several feedbacks from the system. Monitoring the welding process by using the system feedback is an essential procedure during the welding process [18]. Accordingly, the control block diagram is shown in Figure1. The welding torch tip coordinates (U^1_m, V^1_m) are obtained by an image processing algorithm using the feedback images captured from CCD1. The same method is applied to obtain (U^2_m, V^2_m) using the feedback images taken from CCD2. The coordinates of the previous step (U^1_{m-1}, V^1_{m-1}) and (U^2_{m-1}, V^2_{m-1}) are recorded for processing whenever a redirection or a curve occurs. Welding process continues the progress in a direct line until the time a change occurs. In addition, the thickness of the work piece (U_t, V_t) is compared with the system database for possible variation (U_i, V_i). Furthermore, the IR detector will be kept off if the comparison is bigger than 10 millimeters. Otherwise, the feedback pictures of IR detector will be compared with the system database to compute the best distance between the welding torch tip and the seam. The coordinates (u_t, v_t) are captured by CCD1. ΔH, ΔD and ΔT are the image errors computed from images captured by CCD1, CCD2 and IR camera, respectively. These errors are imported to the fuzzy controller.

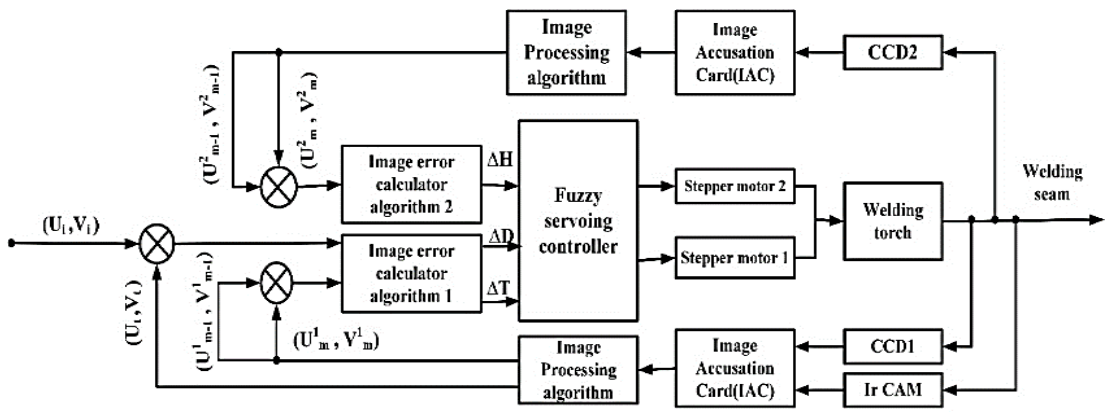

Fig. 1. System block diagram

Because of the lights, weld particles and other noises, it is difficult to capture proper pictures during the welding process. It seems that the welding process should be stopped when a new direction occurs [6]. In this situation, the proposed method estimates the necessary size of redirection in both up-down and left-right directions, continuously. To do this, we applied an image processing algorithm, which obtains the new set-point regarding to the welding seam center. This algorithm detects feature line of the welding seam from the images taken from two CCD cameras. These cameras and IR sensor are mounted on a base frame (shown in figure 2). Based on the errors computed by the image processing algorithms, three data lines are sent to the fuzzy-servoing controller unit. This unit drives the signals of two stepper motors regarding to the error center of the welding seam. Stepper motor1 controls

the welding torch tip in up-down direction, and stepper motor2 controls the welding torch tip in left-right direction.

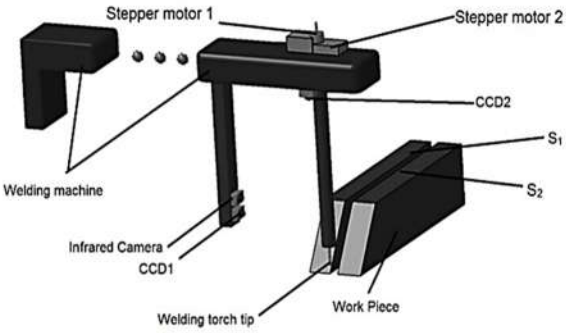

Fig. 2. Schematic view of the welding mechanism with two CCD cameras and an IR camera

3. Visual Seam Detection

Generally, feature detection is the major part of visual systems. In a visual system, the image features are obtained by appropriate image-processing algorithms [16]. Figure 3 gives two image examples taken from CCD1 and CCD2. The seam line and its feature lines are shown in this figure. The images are consisted of two side lines of the welding seam. Image processing algorithm should detect and extract these lines to align the torch tip above the center of the seam.

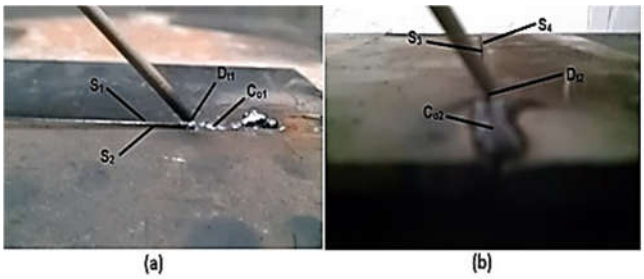

Fig. 3. Demonstrates images captured by CCD cameras. (a) CCD1 (b) CCD2

Two feature lines, S_1 and S_2, are extracted from pictures captured by CCD1. The same feature lines S_3 and S_4 are extracted from pictures captured by CCD2. In order to find the welding seam center, x_0, x_1, x_2, …, x_n and y_0, y_1, y_2, …, y_n guide lines are drawn virtually by the image processing algorithm. Two points, D_1 and D_2, are made by the intersection of the lines x_0,…,x_n with S_1 and S_2 lines, respectively. The same points, D_3 and D_4, are made by intersection of lines y_0, ..., y_n with lines S_3 and S_4, respectively. Lines x_0, …, x_n are perpendicular to the line S_1. And points C_0, C_1, C_2, …, C_n are centers of (D_1D_2) lines in the images captured by CCD1. e_0, e_1 e_2,…, e_n are centers of (D_3D_4) lines in the images captured by CCD2.

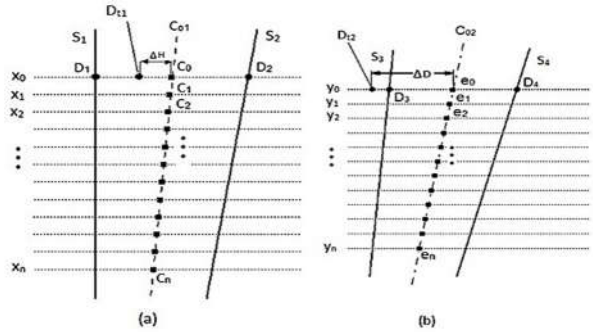

Fig. 4. Image error calculation method. (a) Is representing the feature lines (S_1, S_2) extracted from images captured by CCD1. (b) Is representing the feature lines (S_3, S_4) extracted from images captured by CCD2.

The welding seam center line is shown with C_{o1} and C_{o2} from pictures captured by CCD1 and CCD2, respectively. These lines are created by joining each center point one after another for each line, separately. The positions D_{t1} and D_{t2} of the welding torch tip are obtained from images captured by CCD1 and CCD2, respectively. The distance ΔH is from the center point C_0 to D_{t1}, which is the image error, occurred during the welding process in the images captured by CCD1. And ΔD is the same error in images captured by CCD2. For the best quality of weld joints, ΔH and ΔD should approach to zero. F_{o2} and G_{o2} are coordinates of points C_0, C_1, C_2,…, C_n in images captured by CCD1, which are given in equation(1). (F_{i1}, G_{i1}) and (F_{i2}, G_{i2}) are the coordinates of points D_1 and D_2, respectively. Calculation for image coordinates of points e_0, e_1, e_2,…, e_n in images captured by CCD2 and coordinates of points D_3 and D_4 are similar to equation (1).

$$\begin{cases} F_{o2} = \dfrac{F_{i1} + F_{i2}}{2} \\ G_{o2} = \dfrac{G_{i1} + G_{i2}}{2} \end{cases} \tag{1}$$

For the linear welding seam, the equation of lines C_{o1} and C_{o2} are given in (2) and (3).

$$\begin{cases} (F - F_1) = m(G - G_1) \\ where: m = \tan\left(\dfrac{F_1}{G_1}\right) \end{cases} \tag{2}$$

$$\begin{cases} (U - U_2) = m(V - V_2) \\ where: m = \tan\left(\dfrac{U_2}{V_2}\right) \end{cases} \tag{3}$$

The image errors ΔH and ΔD are calculated using equation (4)

$$\begin{cases} \Delta H = F_{t1} - G_{ci} & i = 1,2,\dots,n \\ \Delta D = F_{t2} - G_{ej} & j = 1,2,\dots,n \end{cases} \tag{4}$$

During the welding process, cross section of welding seam does not usually change. However, it is sometimes necessary to weld a curved seam. In order to find feature lines S_1 and S_2, a different image processing algorithm is required.

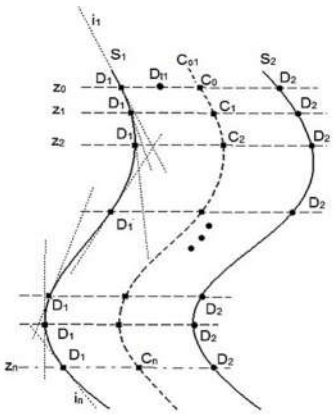

Fig. 5. Feature detection and image error calculation method for the curved welding seam which represents the feature line S1 and S2, for the images captured by CCD1.

In figure 5, lines $i_1 \ldots i_n$ were drawn as tangent lines to feature line of S_1. D_1 points are obtained by the contact point of the tangent lines of $i_1, \ldots, i_n$ with the feature line of S_1. To obtain the point D_2, Lines $z_0, z_1, z_2, \ldots, z_n$ are drawn horizontally to cross D_1 points one after another, and each line passes through the second feature line of S_2. D_1D_2 lines are hypothetical, which were assumed by the image processing algorithm. Centers of D_1D_2 lines are named as $C_0, C_1, C_2, \ldots C_n$. Therefore, C_{o1} is the welding seam center line which is produced by connecting $C_0, C_1, C_2, \ldots C_n$ points to each other, respectively. D_{t1} is the position of the welding torch tip. All of the mentioned image features were obtained from images captured by CCD1; descriptions for images captured by CCD2 are as same. Figure 3 (b) provides the same features by means of CCD2. Image error calculation algorithm is as same as equation (4).

During the welding process, some unexpected noises, such as arc glares, welding splatters and smokes appear which effect on the quality of images captured by CCD cameras. Reflection of arc lights from the camera lens also effects on the image quality [2]. In order to remove these noises, some solutions were addressed in both hardware and software structures of the system [8, 15].

4. Image Processing Principle

In vision-based machinery, image processing is the preliminary part of the design. In order to extract image features, some basic parameters are assigned in the pictures which are called image features. Various image processing software is used by researchers, but MATLAB image processing toolbox is one of the most efficient tools in this field. Additionally, Different algorithms can be applied in this toolbox, the image processing process is fast and accurate. Therefore, in this research we used MATLAB R2014b software to carry out all of the image processing tasks.

Images captured by both CCD cameras are imported to MATLAB (2012b, The MathWorks) [23], then the color images are converted to black and white images. Afterwards, a noise reduction algorithm, Wiener [24] and Median filters [14, 25] were applied to the image to minimize the noise. . The Wiener filter allows us to detect the edge pixels of the weld seam by eliminating the unnecessary glares and sparks. Equations 5, and 6 demonstrate our definition for variant of the classic Wiener filter.

$$A_z(\omega) = \frac{|D_z(\omega)|^2}{|D_z(\omega)|^2 + c\sigma^2} \tag{5}$$

Where,

$$D_z(\omega) = T_0(\omega) - T_z(\omega) \tag{6}$$

The noise variance σ^2 is provided by the noise model and C is a constant accounting for the scaling of the noise variance. T_z emphasized that A_z controls a linear interpolation between T_z and T_0.

On the other hand, Median noise reduction filter is a nonlinear filter, and since its mathematical analysis is complex for images with the random noise, it has to be applied after the Wiener filter. Equations 7 and 8 define the Median noise reduction filter applied in this study.

$$\sigma_{med}^2 = \frac{1}{4nf^2\overline{(n)}} \approx \frac{\sigma_i^2}{n + \frac{\pi}{2} - 1} \cdot \frac{\pi}{2} \tag{7}$$

Where σ_i^2 is the noise variance, n is the median filtering mask's size, $f(\overline{n})$ is the function of the noise density, and the noise variance of the average filtering is

$$\sigma_0^2 = \frac{1}{n}\sigma_i^2 \tag{8}$$

Thereafter, Pattern recognition and line fitting were used for matching the weld joint's feature lines. Hough [26] and canny [27] transforms were applied to detect the feature lines, the edges and corners; the edges of the feature lines are sharper than the other edges in the image. Finally, to define the corners, erosion-dilation technique [28] is used. For the images captured by the IR sensor, we converted color images to the HSV [29] mode to obtain the colors better.

In order to extract feature lines and welding seam center, the noise reduction process is an important part of image processing systems. The hardware instrument noises are removed by two filters. The first is a band-pass filter [19], which removes the reflection noise of the camera lens; the second one is a low-pass filter, which suppresses the light noises that are made by the radiation from melt pool to the camera lens.

5. Strategy of the Visual Fuzzy Controller

In this section, therefore, the structure of the fuzzy system and the controller will be explained. To design the controller system, the distribution of ΔH and ΔD should be computed. Therefore, a membership function is defined over the welding torch tip position with the center of the welding seam. During the welding process, the position of the welding torch tip, with respect to the welding seam, is a key factor for having the best weld quality. As shown in figures 6 through 9, there are four different situations for the fuzzy strategy in the welding process.

The points C_1 and C_2 are the optical centers for CCD1 and CCD2, respectively. T_1 and T_2 are the intersections of the lines C_1T and C_2T with the surface of workpiece, respectively. D_{t1} , D_{t2} , C_{o1} , C_{o2} , $(x_0 \dots x_n)$, $(y_0 \dots y_n)$, S_1 , S_2 , S_3 , S_4 , C_{o1} , C_{o2} , D_1 , D_2 , D_3 , D_4 , c_0 , e_0 are defined previously in figure 5.

5.1. Situation 1

In this situation ΔH=ΔD=0, and it is not necessary to adjust the torch tip. Therefore, the torch tip is exactly at the center of the welding seam, which is the desired position in the welding process. However, in reality, it is not possible to collinear the welding torch tip on the welding seam center accurately. So that, a threshold (Δt) should be defined.

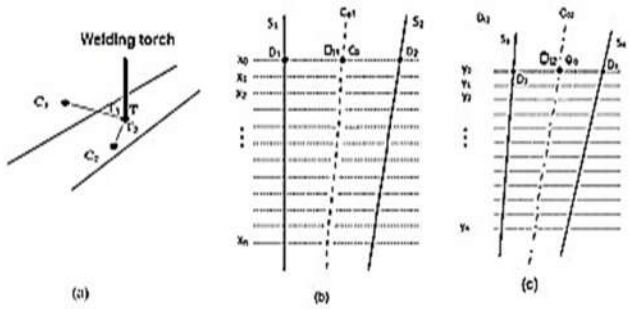

Fig. 6. (Situation 1) The welding torch tip is exactly on the seam center; (a) is the relation between two CCD cameras, welding torch tip and the welding seam; (b) and (c) show feature lines extracted from images captured by CCD1 and CCD2, respectively.

5.2. Situation 2

As shown in figures 7.b and 7.c, it can be seen that the torch tip is on the left side of the welding seam. Therefore, ΔH<0 and ΔD<0, under this situation, welding torch needs to be adjusted to the right side under the given condition.

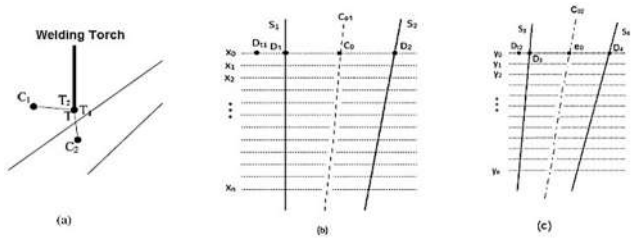

Fig. 7. (Situation 2) The welding torch tip is on the left side of lines $S_1$and S_3; (a) is the relation between two CCD cameras, the torch tip and the welding seam; (b) and (c) show feature lines extracted from images captured by CCD1 and CCD2, respectively.

5.3. Situation 3

In this situation ΔH>0 and ΔD>0 which demonstrate that the torch tip is on the right side of the welding seam and it needs to be adjusted to the left under the given condition.

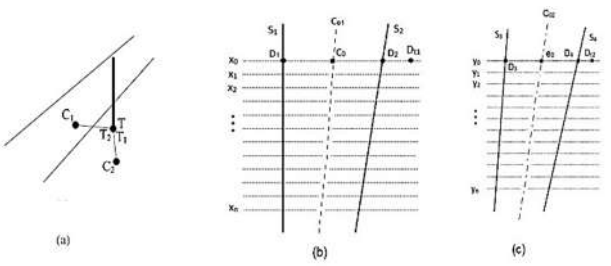

Fig. 8. (Situation 3) The welding torch tip is on the right side of lines S_2 and S_4; (a) is the relation between two CCD cameras, the torch tip and the welding seam; (b) and (c) show feature lines extracted from images captured by CCD1 and CCD2, respectively.

5.4. Situation 4

In this situation ΔH and ΔD are limited as ΔH<0 and ΔD>0. Figure9.a demonstrates that the torch tip should be moved downward and if ΔH>0 and ΔD<0 then it should be adjusted on the reverse side, upward. Based on the position of the torch tip, the vertical distance between welding torch tip and center of the welding seam has to be controlled.

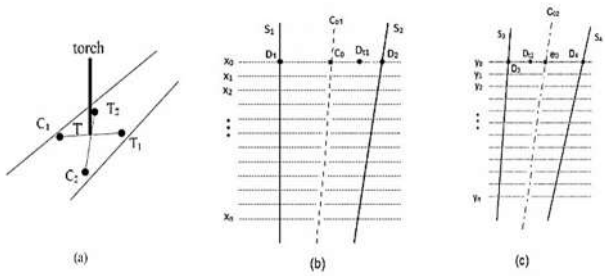

Fig. 9. (Situation 4) The Welding torch tip in the last situation (a) is the relation between two CCD cameras, welding torch tip and the welding seam, (b) and (c) show the feature lines extracted from images captured by CCD1 and CCD2, respectively.

Based on the above configurations, and different situations of the torch tip, movement of the welding torch in two directions (left-right and up-down directions) was controlled. In this research, because of the complexity of the control model and its adaptivity, we applied fuzzy control system using TSK (Takagi-Sugeno and Kang) model [19]. Because the welding system has a constant rate of changes, and also because of the linear dependence of each rule on the system's input variables, a linear system is used. On the other hand, a linear system is appropriate in smooth and accurate movements. Since in linear models, rule activation strength must be high, TSK model is used in this study. Also, the number of rules for decision making in this study is high, and TSK model can make more accurate and real-time decisions. Using a nonlinear model, on the other hand, is not suitable for this application since the torch has to be driven with a constant speed through the seam. In nonlinear systems, the decision-making process is complex and this complexity causes delay in the system and breakage of the weld, which causes weld imperfections such as weld undercut, lack of penetration, solidification cracking, etc. Therefore, a continuous process of welding is a vital factor for the best weld qualities, approving that a linear modeling is a suitable practice in this study.

As shown in figure 1, ΔH and ΔD are two system inputs; the outputs are pulse numbers for the two stepper motors. Most rules have descriptions for inference of the fuzzy controller (shown in equations 9 and 10).

$$R_1^m: \text{IF } \Delta H \text{ is } \Delta\tilde{H} \text{ and } \Delta D \text{ is } \Delta\tilde{D} \text{ and T is } \tilde{T} \quad \text{THEN} \quad P_1^m = a_1^m \Delta H + a_2^m \Delta D \tag{1}$$

$$R_2^m: \text{IF } \Delta H \text{ is } \Delta\tilde{H} \text{ and } \Delta D \text{ is } \Delta\tilde{D} \text{ and T is } \tilde{T} \quad \text{THEN} \quad P_2^m = b_1^m \Delta H + b_2^m \Delta D \tag{2}$$

Where R_1^m and R_2^m represent m-th fuzzy rule of the two systems, when m=1, 2 … 27. System outputs are represented by P_1^m and P_2^m. a_1^m, a_2^m, b_1^m, b_2^m are the model parameters of the fuzzy system and $\Delta\tilde{I}_1$, $\Delta\tilde{I}_2$ and $\tilde{T}$ denote the fuzzy set of ΔH, ΔD and T, respectively.

In situation 4, vertical adjustments are under control. So that, if the thickness of workpiece is too low, the welding torch should be adjusted upward to prevents workpiece melting. In this case, the molten pool temperature is controlled by a Fuzzy controller using IR sensor and the thickness of workpiece. It captures pictures from the molten pool continuously. Then, a comparator compares the captured pictures with a dataset. In order to adjust the welding torch tip position, the fuzzy controller sends appropriate signal ratios to the stepper motor 1.

The membership function of the linguistic variables with distribution of ΔH and ΔD are shown in Fig.10. Where μ(ΔH) and μ(ΔD) are the membership of the input values ΔH and ΔD, respectively.

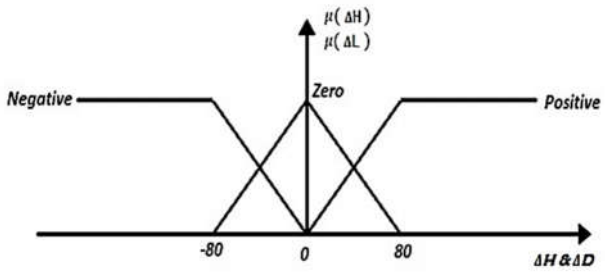

Fig. 10. Membership function of ΔH and ΔD

The membership function of the fuzzy system, based on the distribution of temperature (T), is shown in figure 11, where p(T) is the membership of the input value T.

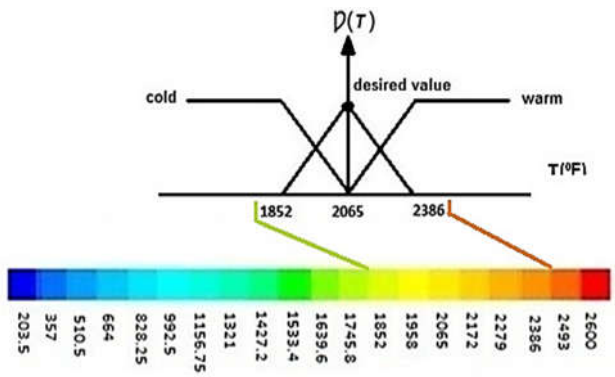

Fig. 11. Membership function of H

Both of two fuzzy systems have eight specific rules, which are shown as below. Some of these rules do not effect on the system. Therefore, they were not mentioned in the calculations.

Table. 1. Fuzzy rules for stepper motor 1 and 2. (a), (b), (c) are Temperatures measured by an IR cam that are cold, desired value and warm, respectively.

R_1^n , R_2^n		ΔH		
		Negative	Zero	Positive
ΔD	Negative	0 , 0	0 , 0	P_1^7,P_2^7
	Zero	P_1^2,P_2^2 *	0 , 0	P_1^8,P_2^8
	Positive	0 , 0	0 , 0	P_1^9,P_2^9

(a) T is cold n=1, 2 … 9

R_1^n , R_2^n		ΔH		
		Negative	Zero	Positive
ΔD	Negative	0 , 0	P_1^{13},P_2^{13}	P_1^{16},P_2^{16}
	Zero	0 , 0	P_1^{14},P_2^{14}	P_1^{17},P_2^{17}
	Positive	0 , 0	P_1^{15},P_2^{15}	P_1^{18},P_2^{18}

(b) T is desired value n=10, 11 … 18

R_1^n , R_2^n		ΔH		
		Negative	Zero	Positive
ΔD	Negative	0 , 0	P_1^{22},0	P_1^{25},0
	Zero	0 , 0	P_1^{23},P_2^{23}	P_1^{26},P_2^{26}
	Positive	0 , 0	P_1^{24},0	P_1^{27},0

(c) T is warm n=19, 20 … 27

Note that: P_1^2, P_2^2 occur in the initial point. And condition of ΔH<0 in all temperatures belongs to the welding initial point which cannot be negative during the welding process. The workpiece Surface is always kept as a reference of welding torch tip which is always zero.

In order to position the torch tip, in the vertical direction with respect to the center of the welding seam, the possible errors were computed. Therefore, the controller computes the necessary pulse number for the stepper motor 1 to guide the torch tip to the desired point (Table 2).

Table. 2. Input pulse number calculated for stepper motor 1

Pulse number	Pulse size
P_1^2	$-\mathrm{sgn}(\Delta H)[1-\mathrm{sgn}(\Delta D)](a_1^2\Delta H+a_2^2\Delta D)$
$P_1^7=P_1^{16}=P_1^{25}$	$\{(-\mathrm{sgn}(\Delta H))[1-\mathrm{sgn}(\Delta H)](\mathrm{sgn}(\Delta D))[1+\mathrm{sgn}(\Delta D)]\}(a_1^7\Delta H+a_2^7\Delta D)$
$P_1^8=P_1^{17}=P_1^{26}$	$\mathrm{sgn}(\Delta D)[1+\mathrm{sgn}(\Delta D)](a_1^8\Delta H+a_2^8\Delta D)$
$P_1^9=P_1^{18}=P_1^{27}$	$\{(\mathrm{sgn}(\Delta H))[1+\mathrm{sgn}(\Delta H)](\mathrm{sgn}(\Delta D))[1+\mathrm{sgn}(\Delta D)]\}(a_1^9\Delta H+a_2^9\Delta D)$
$P_1^{13}=P_1^{22}$	$-\mathrm{sgn}(\Delta H)[1-\mathrm{sgn}(\Delta H)](a_1^4\Delta H+a_2^4\Delta D)$
$P_1^{14}=P_1^{23}$	$\mathrm{sgn}(\Delta D)[1+\mathrm{sgn}(\Delta D)](a_1^5\Delta H+a_2^5\Delta D)$
$P_1^{15}=P_1^{24}$	$\mathrm{sgn}(\Delta H)[1+\mathrm{sgn}(\Delta H)](a_1^6\Delta H+a_2^6\Delta D)$

When a redirection is required in the horizontal, left and right, direction, the amount of redirection is computed by means of the images captured by CCD2. The controller computes the error size and calculates the necessary pulse number for the stepper motor 2 (Table 3). Then, the stepper motor 2 will guide the torch tip to the desired point.

Table. 3. Input pulse number calculated for stepper motor 2

Pulse number	Pulse size
P_2^2	$[1+sgn(\Delta D)](b_1^2\Delta H+b_2^2\Delta D)$
$P_2^7=P_2^{16}$	$[1-sgn(\Delta D)][1+sgn(\Delta H)](b_1^7\Delta H+b_2^7\Delta D)$
$P_2^8=P_2^{17}=P_2^{26}$	$[1-sgn(\Delta D)](b_1^8\Delta H+b_2^8\Delta D)$
$P_2^9=P_2^{18}$	$[1+sgn(\Delta D)][1+sgn(\Delta H)](b_1^9\Delta H+b_2^9\Delta D)$
P_2^{13}	$[1+sgn(\Delta H)](b_1^4\Delta H+b_2^4\Delta D)$
$P_2^{14}=P_2^{23}$	$[1-sgn(\Delta D)](b_1^5\Delta H+b_2^5\Delta D)$
P_2^{15}	$[1-sgn(\Delta H)](b_1^6\Delta H+b_2^6\Delta D)$

In order to define the accurate pulse number for each stepper motor, different variables have to be defined, which are called model variables. Table 4 defines the model parameters for the fuzzy controller to control each stepper motor individually.

Table. 4. Model parameter of each CCD camera, (a) demonstrates the model parameters a_1 and a_2 for CCD1. (b) Demonstrates the model parameters b_1 and b_2 for CCD 2.

(a_1^m, a_2^m)		Negative	Zero	Positive
	Negative	8, 8	4, 2	0, 0
	Zero	2, 4	0, 0	2, 4
	Positive	0, 0	4, 2	8, 8

(a)

(b_1^m, b_2^m)		Negative	Zero	Positive
	Negative	0, 0	2, -1	7, -7
	Zero	-1, 2	0, 0	1, -2
	Positive	-7, 7	-2 , 1	0, 0

(b)

Up-down and left-right stepper motors are controlled by the number of input pulses of P_1 and P_2. And they are calculated as shown in equations (9) and (10).

$$P_1 = \frac{\sum_{m=1}^{27} \omega^m P_1^m}{\sum_{m=1}^{27} \omega^m} \tag{9}$$

$$P_2 = \frac{\sum_{m=1}^{27} \omega^m P_2^m}{\sum_{m=1}^{27} \omega^m} \tag{10}$$

Where ω^m is the firing strength of the m-th fuzzy rule, which is given in equation (11).

$$\omega^m=\mu^m\Delta\tilde{H}(\Delta H)\mu^m\Delta\tilde{D}(\Delta D)p^m\tilde{H}(H) \tag{11}$$

In equation (11), $\mu^m\Delta\tilde{H}(\Delta H)$, $\mu^m\Delta\tilde{D}(\Delta D)$ and $p^m\tilde{T}(T)$ are the membership of ΔH, ΔD and T which belong to $\Delta\tilde{H}$, $\Delta\tilde{D}$ and $\tilde{T}$ in the m-th fuzzy rule, respectively.

Since this welding machine is capable to perform the welding process on various work pieces, it can be applied to most of the welding projects. Construction skeleton is one of the situations that this welding mechanism can be applied on. Furthermore, the robot benefits two cameras which are taking pictures permanently. The images are stored and can be used for any further considerations and investigations about the weld quality and the whole process.

6. Experimental and Analytical Results

In this section, the results of experiments are presented. In order to carry out the experiments, a V-shaped straight welding seam was welded, in which width, depth and length were considered 2mm, 20mm and 500mm, respectively. The workpiece material is 5086 aluminum alloy. In order to make a real-time structure, a high-speed control processing unit (CPU) and extra memory storage are used. Therefore, we ran the image processing algorithm and the controller on a computer with 2.40GHz Core-Duo2 processor and 4GB of memory. The image processing rate was approximately 2 images per second.

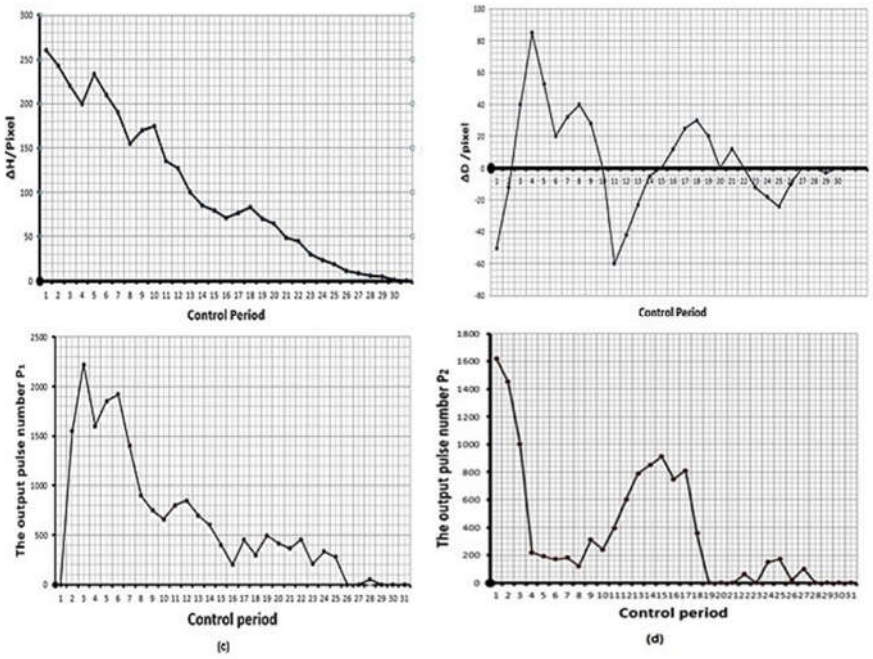

Fig. 12. Experimental results (a) And (b) are image errors detected by CCD1 (ΔH) and CCD2 (ΔD), respectively, (c) and (d) are the calculated output pulse numbers P_1 and P_2, respectively.

In this experiment, the control period was 30ms and the model parameters (a_1^m, a_2^m, b_1^m, b_2^m) are given in table 4. At the beginning of the experiment, welding torch was adjusted to a random point, which was in the lower-right section of the welding seam center. ΔH and ΔD were measured in the images captured by CCD 1 and CCD2, which are about -4 and -2, respectively. As shown in the diagrams in Fig.12 (a) and (c). The output control pulses were extracted during the control period (Fig.12 (b) and (d)). In this study since two CCD cameras have been applied to the system, the welding manipulation is carried out with a great precision. The torch tip is placed on the exact location with respect to the seam. On the other hand, the IR detector monitors the weld pool temperature continuously, not allowing the workpiece to melt. During the calibration and without considering the image processing errors, measurements show that the system error was almost 0.5mm × 0.5mm in both directions, which can be concluded that the system meets the requirements for the welding application.

7. Conclusion

In this research an automatic real-time welding system was proposed. In this system, auto alignment of the welding torch tip with the center of the welding seam at the initial point was controlled by fuzzy rules. The rules are based on the T-S fuzzy model, and two sets of equations were written for the system controller unit. In this system, an IR sensor is used to check the temperature of the weld pool. An image processing algorithm, by means of images captured from two CCD cameras, extracts the position of the welding torch tip with respect to the welding seam. These Images can be also used by a weld inspector to inspect and monitor the welding quality. Experimental results and pictures demonstrate that the proposed system meets the quality requirements. The errors in height (ΔH) and in width (ΔD) are achieved to desired value of (Δt) in less than 30ms, which guaranties the accuracy of the control system that performs the automated welding process.

For the future research, we would like to use a line following method with stereo vision technique based on the fuzzy control rules in the arc welding process.

Acknowledgment

This work was supported by the Mechatronic Research Laboratory (MRL) of Qazvin Islamic Azad University (QIAU).

References

[1] Yan, Z.; Xu, D.; Li, Y., "A visual servoing system for the torch alignment to initial welding position". In International Conference on Intelligent Robotics and Applications. Springer. (2008).

[2] Park, K.; et al., "Development of an auto-welding system for CRD nozzle repair welds using a 3D laser vision sensor". Journal of mechanical science and technology. 21(10): pp. 1720-1725 (2007).

[3] Li, Y.; et al., "Measurement and defect detection of the weld bead based on online vision inspection". IEEE Transactions on Instrumentation and Measurement. 59(7): pp. 1841-1849 (2010).

[4] Vimal, K.; Vinodh, S.; Raja, A., "Modelling, assessment and deployment of strategies for ensuring sustainable shielded metal arc welding process–a case study". Journal of Cleaner Production. 93: pp. 364-377 (2015).

[5] Shah, H.M.; et al., "Vision Based Identification and Detection of Initial, Mid and End Points of Weld Seams Path in Butt-Welding Joint using Point Detector Methods". Journal of Telecommunication, Electronic and Computer Engineering (JTEC). 8(7): pp. 57-61 (2016).

[6] Gargaud, M.; Amils, R.; Cleaves, H.J., "Encyclopedia of anthropology". Springer Science & Business Media. Vol. 1. (2011).

[7] Chen, H.; Xu, D.; Wang, H., "Three dimension curve welding seam modeling for seam tracking". IFAC Proceedings Volumes. 41(2): pp. 9186-9191 (2008).

[8] Xu, D.; et al., "Compact visual control system for aligning and tracking narrow butt seams with CO2 gas-shielded arc welding". The International Journal of Advanced Manufacturing Technology. 62(9-12): pp. 1157-1167 (2012).

[9] Chokkalingham, S.; Chandrasekhar, N.; Vasudevan, M., "Predicting the depth of penetration and weld bead width from the infrared thermal image of the weld pool using artificial neural network modeling". Journal of Intelligent Manufacturing. 23(5): pp. 1995-2001 (2012).

[10] Le, J.; Zhang, H.; Xiao, Y., "Circular fillet weld tracking in GMAW by robots based on rotating arc sensors". The International Journal of Advanced Manufacturing Technology. 88(9-12): pp. 2705-2715 (2017).

[11] Zhu, Z.Y.; et al., "Recognition of the initial position of weld based on the image pattern match technology for welding robot". The International Journal of Advanced Manufacturing Technology. 26(7-8): pp. 784-788 (2005).

[12] Chen, X.; et al., "Practical method to locate the initial weld position using visual technology". The International Journal of Advanced Manufacturing Technology. 30(7-8): pp. 663-668 (2006).

[13] Satheesh, M.; Dhas, J.E.R., "Multi objective optimization of flux cored arc weld parameters using fuzzy based desirability function". Iranian Journal of Science and Technology. Transactions of Mechanical Engineering. Vol. 37 (2), pp. 175-187 (2013).

[14] Wang, X.; et al., "Groove-center detection in gas metal arc welding using a template-matching method". The International Journal of Advanced Manufacturing Technology, pp. 1-11 (2016).

[15] Zhou, L.; Lin, T.; Chen, S.-B., "Autonomous acquisition of seam coordinates for arc welding robot based on visual servoing". Journal of Intelligent and Robotic Systems, 47(3): pp. 239-255 (2006).

[16] Yan, Z.; et al., "A vision-based seam tracking system for submerged arc welding, in Robotic Welding, Intelligence and Automation". Springer. pp. 349-357 (2007).

[17] Shen, H.-y.; et al., "Arc welding robot system with seam tracking and weld pool control based on passive vision". The International Journal of Advanced Manufacturing Technology. 39(7-8): pp. 669-678 (2008).

[18] Bazargan-Lari, Y.; et al., "Adaptive feedback linearization tracking of an scara gas metal arc welding robot in a cascade structure", in proceedings of the ASME 2011 International Mechanical Engineering Congress & Exposition IMECE (2011).

[19] Xu, P.; et al., "A visual seam tracking system for robotic arc welding". The International Journal of Advanced Manufacturing Technology, 37(1-2): pp. 70-75 (2008).

[20] Gao, X.; You, D.; Katayama, S., "Infrared image recognition for seam tracking monitoring during fiber laser welding". Mechatronics, 22(4): pp. 370-380 (2012).

[21] Dong, G.; Zhu, Z., "Position-based visual servo control of autonomous robotic manipulators". Acta Astronautica, 115: pp. 291-302 (2015).

[22] Kuljić, B.; Simon, J.; Szakáll, T. "Pathfinding based on edge detection and infrared distance measuring sensor". Acta Polytechnica Hungarica, vol. 6 (1) (2009).

[23] MATLAB, M.-V., 8.0. 0.783 (R2012b). Natick, Massachusetts: The MathWorks Inc, 82 (2012).

[24] Aminzadeh, M.; Kurfess, T., "A novel background subtraction technique based on gray-scale morphology for weld defect detection. In SPIE Smart Structures and Materials+ Nondestructive Evaluation and Health Monitoring". International Society for Optics and Photonics (2016).

[25] Zhang, G.; Wu, C.S.; Liu, X., "Single vision system for simultaneous observation of keyhole and weld pool in plasma arc welding". Journal of Materials Processing Technology. 215: pp. 71-78 (2015).

[26] Huang, W.; Kovacevic, R., "Development of a real-time laser-based machine vision system to monitor and control welding processes". The International Journal of Advanced Manufacturing Technology. 63(1-4): pp. 235-248 (2012).

[27] Yan, Z.; Xu, D., "Visual tracking system for the welding of narrow butt seams in container manufacture", in Proceedings of the UKACC International Conference on Control (2008).

[28] Sung, K.; et al., "Development of a multiline laser vision sensor for joint tracking in welding". The Welding Journal. 4: pp. 79-85 (2009).

[29] Muhammad, J.; Altun, H.; Abo-Serie, E., "Welding seam profiling techniques based on active vision sensing for intelligent robotic welding". The International Journal of Advanced Manufacturing Technology, pp. 1-19 (2016).